Hexagonal optical structures in photorefractive crystals with a feedback mirror

P. M. Lushnikov*)

L. D. Landau Institute of Theoretical Physics, Russian Academy of Sciences, 117334 Moscow, Russia
(Submitted 13 October 1997)
Zh. Éksp. Teor. Fiz. **113**, 1122–1146 (March 1998)

A nonlinear theory is presented for the formation of hexagonal optical structures in a photorefractive medium equipped with a feedback mirror. Oppositely directed beams in photorefractive crystals are unstable against the excitation of sideband waves. It is shown here that as this instability evolves to its nonlinear stage, the three-wave interaction between weak sideband beams does not stabilize it, but rather leads to explosive growth of the amplitudes of beams whose transverse wave vectors form angles that are multiples of $\pi/3$. As a result, sideband beams at these angles are found to be correlated. A range of parameters is found in which four-wave interactions saturate the explosive instability, which explains the appearance of stable hexagons in the experiment. Outside this region, nonlinearities of higher order saturate the explosive instability, and the process of hexagon generation must be studied numerically. Matrix elements are obtained for the three- and four-wave interactions as functions of the distance to the feedback mirror, and an equation for the time evolution of the sideband wave amplitudes is derived that describes the hexagon generation. A comparison is made with experimental results for the photorefractive crystals $KNbO_3$ and $BaTiO_3$. © *1998 American Institute of Physics.* [S1063-7761(98)02903-5]

1. INTRODUCTION

Oppositely directed optical beams passing through nonlinear media often exhibit transverse instability against the excitation of waves at small angles to the primary propagation direction and the generation of transverse hexagon-shaped optical structures.[1–5] This instability is caused by positive feedback between the counterpropagating beams, and is absolute in nature. In photorefractive crystals such phenomena have been especially well-studied,[6–9] due to the extreme ease with which the evolution of the transverse instability and formation of regular structures can be observed. Characteristic times for the creation of these structures range from tenths to tens of seconds. Typical nonlinear lengths within these crystals, over which the amplitude of the light beams changes appreciably, are several millimeters, and the intensities of the pump beams required to generate them are achievable using cw lasers.[10]

Until recently, theoretical studies of the transverse instability concentrated mostly on calculating threshold conditions for the generation of transverse optical structures. This was first done for Kerr media,[11] followed by threshold calculations for the photorefractive crystals $KNbO_3$ and $BaTiO_3$ equipped with feedback mirrors,[12] and the crystals $LiNbO_3$ and $LiTaO_3$ illuminated by oppositely directed pump beams but with no feedback mirror.[13] The crystals $KNbO_3$ and $BaTiO_3$ are the best ones to study from an experimental point of view. When these crystals are equipped with feedback mirrors, it is found that stationary hexagonal structures form, with an instability threshold that is in rather good agreement with theoretical predictions.[6,8,12] In Ref. 12, Honda and Banerjee found the threshold by assuming that the instability was aperiodic, i.e., the imaginary part of the instability growth rate equaled zero at the threshold of the instability (if this were not the case, moving optical structures would be seen. Experimentally, such a motion can only be produced by mismatching the directions of the oppositely directed beams slightly). In other words, the frequency detuning between pump and sideband waves is assumed to be zero at the instability threshold.

Above threshold, the instability leads to generation of weak optical beams at small angles $\theta=|\mathbf{k}_\perp|/k_0$ to the pump beams, where k_0 is the wave vector of the pump beams and $|\mathbf{k}_\perp|$ is the transverse component of the excitation beam wave vector. For pumping slightly above threshold, the only beams generated had wave vectors in a narrow layer around $|\mathbf{k}_\perp|\simeq k_{0\perp}$, where the instability growth rate is a maximum (here $k_{0\perp}$ is the value of the transverse wave vector corresponding to maximum gain). Thus, the initial stage of the evolution of the instability involves the creation of annular structures (in the plane perpendicular to the pump beam) with amplitudes that decay exponentially with time. The distribution of intensity along the beam at this stage is arbitrary and is determined by fluctuations in the medium. This theory is linear in the amplitudes of the weak beams, and therefore cannot describe the subsequent evolution of the instability which leads to the formation of regular hexagonal optical structures. These structures arise from nonlinear interactions between the weak optical beams. The task of this paper is to derive a theory of this interaction for photorefractive $KNbO_3$ and $BaTiO_3$ crystals equipped with a feedback mirror. The small parameter used in the theory is the amplitude of the sideband waves normalized by the square root of the intensity of the pump beams. Since the instability is aperiodic, three-wave interactions between optical beams whose transverse wave vectors make angles with each other that are

multiples of $\pi/3$ become important as the instability evolves toward its nonlinear stage. It is shown here that this interaction does not stabilize the instability, but rather leads to explosive growth in the amplitudes of the weak sideband waves, as a result of which hexagonal structures form. This can be understood from the following example. Let us assume that as a result of the evolution of the linear instability three weak beams are excited with wave vectors $\mathbf{q}_j=(k_0,\mathbf{k}_{\perp j})$, $j=1,2,3$, equal real amplitudes A, and transverse wave vectors $\mathbf{k}_{\perp j}$ that make angles of $\pi/3$ with each other. The linear instability theory of Ref. 12 implies that three other beams with the transverse wave vector $-k_{\perp j}$ will also be excited in the system at the same time, and six beams with $-k_0$: $\mathbf{q}=(-k_0,\pm\mathbf{k}_{\perp 1,2,3})$. The amplitudes of these waves all equal A.

It will be show below that the evolution of $A(t)$ is determined by the following equation:

$$\frac{\partial A}{\partial t}=\nu_0 A+UA^2, \tag{1}$$

where $\nu_0=\nu_{k_{0\perp}}$ is the instability growth rate at its maximum point $|k_\perp|=k_{0\perp}$ and U is the matrix element for the three-wave interaction. Setting $A|_{t=0}=A_0$ and integrating this equation gives

$$A=\frac{A_0\nu_0}{(\nu_0+UA_0)e^{-\nu_0 t}-UA_0}, \tag{2}$$

This expression reveals that there exists a time $t_{\rm cr}>0$ at which the amplitude A goes to infinity when the condition $A_0U>0$ holds. This is an example of a so-called explosive instability, for which the solution becomes singular at a finite time. Thus, a fundamental feature of this problem is that three-wave processes lead to correlations between perturbations whose transverse wave vectors $\mathbf{k}_\perp$ make angles with one another that are multiples of $\pi/3$. These correlated perturbations generate hexagons in the plane of transverse wave vectors $\mathbf{k}_\perp$. In this case there is no correlation between different hexagons, and the interaction between them is small. Four-wave and higher-order wave processes stabilize the instability, and also suppress the generation of other hexagons with smaller amplitudes (i.e., those hexagons which begin to grow after the primary one). Thus, hard excitation of hexagons takes place until amplitudes are reached at which the excitation is stabilized by nonlinearities of fourth and higher order. This hard excitation of hexagons is the analog of a first-order phase transition.

A more general equation, which describes the evolution of weak beams A_k with transverse wave vector $\mathbf{k}$, will be derived below (here and below the sign $\perp$ will be omitted), taking into account three- and four-wave interactions:

$$\frac{\partial A_k}{\partial t}=\nu_0 A_k+\frac{1}{2}\,U\sum_{\mathbf{k}_1+\mathbf{k}_2=\mathbf{k}}A_{k_1}A_{k_2} - \frac{1}{3!}\sum_{\mathbf{k}_1+\mathbf{k}_2+\mathbf{k}_3=\mathbf{k}}T_{-k\,k_1k_2k_3}A_{k_1}A_{k_2}A_{k_3}, \tag{3}$$

where U, $T_{-kk_1k_2k_3}$ are the matrix elements of the three- and four-wave processes evaluated on the surface $|\mathbf{k}|=k_{0\perp}$. Since linear instability theory predicts the growth of perturbations within the thin ring $|\mathbf{k}|\simeq k_{0\perp}$, in summing in Eq. (3) it is sufficient to retain only those transverse wave vectors whose magnitude corresponds to the maximum linear growth rate, i.e., $|\mathbf{k}|=k_{0\perp}$. Thus, Eq. (3) is essentially a Laudau expansion in the amplitude A_k of the growing linear modes (see, e.g., Ref. 14).

Note that the applicability of Eq. (3), i.e., the possibility of limiting the treatment to three- and four-wave processes, assumes that the nonlinearity is small. For this to be true in general, the matrix element U is required to be small independent of how far above threshold the system is. In the theory of phase transitions this corresponds to a first-order phase transition that is close to a second-order phase transition by virtue of the smallness of the order parameter discontinuity. In photorefractive crystals, the matrix element U is not particularly small; however, the matrix element $T_{-kk_1k_2k_3}$ contains a rather large numerical factor which justifies the existence of a range where Eq. (3) is applicable whenever the total contribution of four-wave processes can provide both saturation of the explosive instability and stability of the stationary hexagonal lattices. In what follows, a range of parameters will be found in which such saturation and stability are actually achieved, and the results of analytic four-wave theory will be compared with a numerical experiment that takes into account wave processes of higher order. As a result, it will be shown that the analytic theory describes the process of hexagon generation in a qualitatively correct manner, but that the stationary amplitudes it predicts differ by roughly a factor of 2 from those obtained by the numerical experiment. Thus, higher-order wave processes lead to an important renormalization of the hexagon amplitudes. The numerical calculations also show that when a range of parameters is deliberately chosen for which four-wave theory cannot saturate the explosive instability, the hexagons are stabilized at larger amplitudes, i.e., for stronger nonlinearity.

The plan of this paper is as follows: in Sec. 2 nonlinear equations are derived that describe the evolution of sideband beams in photorefractive media with a feedback mirror, and a general boundary value problem is formulated for solving these equations. In Sec. 3 the linear theory of transverse instability is investigated by linearizing this boundary value problem. As a result, the threshold condition is found for the instability, along with eigenvectors for the direct and Hermitian-conjugate linear boundary value problems. In Sec. 4 expressions are obtained for the matrix element U of the three-wave interaction. The fact that this matrix element will turn out to be nonzero is of fundamental importance. In Sec. 5 the overall amplitude equation (3) is derived, along with an expression for the four-wave interaction matrix element $T_{-kk_1k_2k_3}$. For photorefractive crystals like $KNbO_3$ and $BaTiO_3$, the matrix elements U and $T_{-kk_1k_2k_3}$ turn out to be purely real. In Sec. 6 an equation is found that describes the time evolution of the hexagon intensity, and the hexagon stability is investigated. This analysis makes it possible to determine the range of parameters in which the four-wave interaction is sufficient to stabilize the growth of the hexagons. In Sec. 7 the generation of hexagons is investigated

numerically, taking into account higher-order nonlinearities, and the theoretical results are compared with experimental results for the photorefractive crystals $KNbO_3$ and $BaTiO_3$. In the last section, all of these results are summarized.

2. FUNDAMENTAL EQUATIONS

Assume that a pump light wave $F_0 \exp[i(n_0k_0z-\omega_0t)]$ propagates along the z axis in a photorefractive crystal along with an oppositely directed wave $B_0 \exp[-i(n_0k_0z-\omega_0t)]$ arising from reflection by a feedback mirror. Here $F_0(z)$, $B_0(z)$ are complex wave amplitudes that vary slowly with z, k_0 is the wave vector of the light waves in vacuum, ω_0 is their frequency, and n_0 is the index of refraction of the crystal. For simplicity we will refer to both waves as pump waves. We denote the distance between the back face of the crystal and the feedback mirror by L and the length of the crystal along the z axis by l, and set the coordinate of the front face of the crystal $z=0$ (see also the experiment setup in Refs. 8 and 12). Consider perturbations of the pump beams in the form of weak sideband waves, and write the total amplitudes of the beams in the form

$$\begin{aligned} F\ \exp[i(n_0k_0z-\omega_0t)] &= F_0\ \exp[i(n_0k_0z-\omega_0t)] \\ &\times\left[1+\sum_{\mathbf{k}}\ \exp(i\mathbf{k}\cdot\mathbf{r}_\perp)F_k(z,t)\right], \\ B\ \exp[-i(n_0k_0z-\omega_0t)] &= B_0\ \exp[-i(n_0k_0z-\omega_0t)] \\ &\times\left[1+\sum_{\mathbf{k}}\ \exp(i\mathbf{k}\cdot\mathbf{r}_\perp)B_k(z,t)\right], \end{aligned} \tag{4}$$

where $\mathbf{k}=(k_x,k_y)$ is the transverse wave vector in the xy plane, $\mathbf{r}_\perp$ is the spatial coordinate in this plane, and F_k, B_k are amplitudes of the sideband waves normalized by the amplitudes of the pump waves. Assume that the polarizations of all the waves are the same, the amplitudes of the sideband waves are small, i.e., $|F_k|$, $|B_k|\ll 1$, and that $|\mathbf{k}|\ll n_0k_0$, i.e., the sideband waves propagate at small angles to the pump beams.

The wave beams in the photorefractive medium interact via the following mechanism. Under the action of the light, current carriers are excited and the crystal acquires a photoconductivity. The modulation of the light intensity caused by interference of the light beams leads to modulation of the photoconductivity and the appearance of a space-charge electric field. Modulation of this space-charge field E in turn leads to modulation of the dielectric constant of the crystal, $\epsilon=\epsilon_0+\delta\epsilon$ according to the linear electrooptic effect: $\delta\epsilon=-n_0^4rE$, where n_0 is the index of refraction of the crystal and r is the effective electrooptic coefficient.[10,15] In particular, if the z axis coincides with the crystallographic z axis, then $r=r_{13}$. Note that only the longitudinal z-component $E\equiv E_z$ of the space-charge field is included in the analysis that follows, since the other components give rise to negligibly small contributions. Thus, the interaction between the light beams arises from their diffraction by the refractive index modulations they induce in the crystal.[10,15]

In this paper we will assume that the wave interaction is mediated only by generation of reflecting refractive index gratings, whose wave vectors are close to $\pm 2n_0k_0$. Under the conditions of the experiment in which the hexagons were seen, interaction via transmission gratings is negligibly small.[8,12] Therefore, the space-charge field $E(\mathbf{r}_\perp,z,t)$ can be written in the form

$$\begin{aligned} E(\mathbf{r}_\perp,z,t) &= \exp(2in_0k_0z)E_{2k_0} \\ &\times\left(1+\sum_{\mathbf{k}}\ \exp(i\mathbf{k}\cdot\mathbf{r}_\perp)E_{2k_0,k}\right) \\ &+\exp(-2in_0k_0z)E_{-2k_0} \\ &\times\left(1+\sum_{\mathbf{k}}\ \exp(i\mathbf{k}\cdot\mathbf{r}_\perp)E_{-2k_0,k}\right), \end{aligned} \tag{5}$$

where $E_{\pm 2k_0}(z)$ are the space-charge field amplitudes arising from the pump beams and $E_{\pm 2k_0,k}(z,t)$ are the space-charge field amplitudes of the sideband beams normalized by the pump-beam field amplitudes. These amplitudes are written by the pump and sideband waves, and also by pairs of weak sideband waves. The reality of the quantity $E(\mathbf{r}_\perp,z,t)$ leads to the following relations between these amplitudes:

$$E_{-2k_0}=E_{2k_0}^*, \quad E_{-2k_0,-k}=E_{2k_0,k}^*.$$

The wave amplitudes F and B vary with time on a scale that is the same order as the characteristic relaxation time of the space-charge field E, which in photorefractive crystals can range from tenths of seconds to tens of seconds;[10] therefore, this dependence can be neglected in the wave equation.[10,15] The equations for the amplitudes F and B, which are slowly varying in z, take the following form in light of Eq. (5):

$$\begin{aligned} \left(\frac{d}{dz}-\frac{i}{2k_0n_0}\,\Delta_\perp\right)F &= -\frac{ik_0n_0^3r}{2}\,BE_{2k_0} \\ &\times\left(1+\sum_{\mathbf{k}}\ e^{i\mathbf{k}\cdot\mathbf{r}_\perp}E_{2k_0,k}\right), \\ \left(\frac{d}{dz}+\frac{i}{2k_0n_0}\,\Delta_\perp\right)B &= \frac{ik_0n_0^3r}{2}\,FE_{-2k_0} \\ &\times\left(1+\sum_{\mathbf{k}}\ e^{i\mathbf{k}\cdot\mathbf{r}_\perp}E_{-2k_0,k}\right), \end{aligned} \tag{6}$$

where $\Delta_\perp=\partial^2/\partial x^2+\partial^2/\partial y^2$.

When the amplitudes of the sideband waves can be neglected, the following expressions for the pump beams follow from Eqs. (6) and (4):

$$\begin{aligned} \frac{d}{dz}\,F_0 &= -\frac{ik_0n_0^3r}{2}\,B_0E_{2k_0}, \\ \frac{d}{dz}\,B_0 &= \frac{ik_0n_0^3r}{2}\,F_0E_{-2k_0}. \end{aligned} \tag{7}$$

Equations (6), (7) must be supplemented by a relation between the space-charge field E and the wave amplitudes. As shown above, the photorefractive nonlinearity is extremely slow; therefore, the generation of the space-charge field turns out to be affected only by the total intensity of the

optical beams averaged over the rapid oscillations with frequency ω_0, i.e., the standing-wave optical patterns formed by interference between the oppositely directed beams. Let us write the light intensity I averaged over the rapid temporal oscillations in the form

$$I=I_\Sigma[I_0+\exp(2in_0k_0z)I_{2k_0}+\exp(-2in_0k_0z)I_{-2k_0}], \tag{8}$$

where

$$\begin{aligned} I_0=&\frac{1}{I_\Sigma}\left\{|F_0|^2\left[1+\sum_{\mathbf{k}} e^{i\mathbf{k}\cdot\mathbf{r}_\perp}(F_k+F^*_{-k})\right.\right.\\ &\left.+\sum_{\mathbf{k}_1,\mathbf{k}_2} e^{i(\mathbf{k}_1+\mathbf{k}_2)\cdot\mathbf{r}_\perp}F_{k_1}F^*_{-k_2}\right]+|B_0|^2\left(1+\sum_{\mathbf{k}} e^{i\mathbf{k}\cdot\mathbf{r}_\perp}(B_k\right.\\ &\left.\left.+B^*_{-k})+\sum_{\mathbf{k}_1,\mathbf{k}_2} e^{i(\mathbf{k}_1+\mathbf{k}_2)\cdot\mathbf{r}_\perp}B_{k_1}B^*_{-k_2}\right)\right\},\\ I_{2k_0}=&\frac{F_0B_0^*}{I_\Sigma}\left[1+\sum_{\mathbf{k}} e^{i\mathbf{k}\cdot\mathbf{r}_\perp}(F_k+B^*_{-k})\right.\\ &\left.+\sum_{\mathbf{k}_1,\mathbf{k}_2} e^{i(\mathbf{k}_1+\mathbf{k}_2)\cdot\mathbf{r}_\perp}F_{k_1}B^*_{-k_2}\right], \end{aligned} \tag{9}$$

here $I_{-2k_0}=I^*_{2k_0}$, and $I_\Sigma=|F_0|^2+|B_0|^2$ is the sum of the pump beam intensities.

Assume that the photorefractive crystal contains a set of donor and acceptor levels with densities N_D and N_A, and densities of ionized donors and conduction-band electrons N_D^+ and n respectively.[16] The compensating acceptor levels are completely occupied by electrons and do not participate in any transitions, and $N_D>N_A$. Let us neglect thermal transitions of electrons from donor levels into the conduction band. Then the acceptor charge $-eN_A$ entirely compensates the charge due to ionized donors in the dark. Assume that phototransitions take electrons from donor levels to the conduction band with a probability $sI(N_D-N_D^+)$, and that electrons are trapped by ionized donors with a probability $g_0N_D^+n$, where s is the photoionization cross section and g_0 is the recombination coefficient. Then the density of ionized donors is given by the equation

$$\frac{\partial N_D^+}{\partial t}=sI(N_D-N_D^+)-g_0N_D^+n, \tag{10}$$

which must be supplemented by the Poisson equation

$$\text{div } E=4\pi\frac{e}{\epsilon_\parallel}(N_D^+-N_A-n) \tag{11}$$

and the equation of continuity

$$\frac{\partial(N_D^+-n)}{\partial t}+\frac{1}{e}\text{ div } j=0, \tag{12}$$

Here $\epsilon_\parallel$ is the static dielectric constant along the z axis. Note that it is sufficient to take into account only the longitudinal dielectric constant, since only small-angle perturbations $|\mathbf{k}|\ll n_0k_0$ are treated in this paper. This in turn implies that it is sufficient to take into account only the longitudinal component $E=E_z$ of the space-charge field. The electric current density j is determined by drift and diffusion of electrons:

$$j=e\mu nE+eD\nabla n, \tag{13}$$

where μ is the carrier mobility, $D=\mu k_BT/e$ is the diffusion coefficient, T is the temperature, and k_B is the Boltzmann constant. In the majority of experiments on excitation of hexagons in photorefractive crystals, conditions are such that N_D, N_D^+, N_A, $|N_D-N_A|\gg n$;[10] furthermore, the characteristic recombination time $1/g_0N_A$ for carriers (electrons) is considerably smaller than the characteristic relaxation time $t_d=\epsilon_\parallel g_0N_A/4\pi e\mu sI_\Sigma(N_D-N_A)$ for the space-charge field. Therefore, the time derivative in Eq. (10) can be neglected, and n can be expressed as a function of the light intensity as follows:

$$n=\frac{sI(N_D-N_A)}{g_0N_A}. \tag{14}$$

From Eqs. (11)–(14) we obtain an equation for the space-charge field:[13,15]

$$I_\Sigma t_d\frac{\partial E}{\partial t}=-\widetilde{IE}-E_{sc}\widetilde{I}, \tag{15}$$

where the tilde instructs us to separate out the spatially oscillating parts with wave vectors $\pm2n_0k_0$. Here $E_{sc}=2in_0k_0D/\mu$ is a characteristic photoinduced electric field that depends only on the properties of the crystal,[15,17] and is caused by diffusion of photoelectrons. If the conductivity of the crystal is predominantly due to holes, we need only change the coefficients that multiply t_d and E_{sc}.[10]

Equations (15), (8), (9) imply the following expression for the amplitude $E_{\pm2k_0}$ of the reflecting grating created by the space-charge field generated by the pump beams:

$$E_{2k_0}=-E_{sc}\frac{F_0B_0^*}{I_\Sigma},\quad E_{-2k_0}=E^*_{2k_0}. \tag{16}$$

The theory presented above is entirely suitable for treating the crystals $KNbO_3$ and $BaTiO_3$ under investigation in this paper. This is because diffusion of photoelectrons dominates in these crystals, and according to Eq. (16) the spatial modulation of the refractive index is shifted by $\pi/2$ relative to the modulation of the standing optical pattern, which corresponds to the so-called nonlocal photorefractive response.[10,17] Note that inclusion of either an applied external electric field or the photogalvanic effect leaves the form of Eq. (15) unchanged, only changing the constant E_{sc}.[15,17] In particular, the quantity E_{sc} is almost real in the crystals $LiNbO_3$ and $LiTaO_3$; therefore, there is no phase shift, which corresponds to the local response caused by drift of electrons in an external field or by the photogalvanic effect.[13,15] Therefore, in the interest of greater generality it is assumed below that E_{sc} is an arbitrary complex constant.

Let us assume that the feedback mirror has unit reflection coefficient, $R=1$, and that the reflection of the light beam from the crystal face is negligibly small. Then we obtain from Eqs. (7) and (16)

$$F_0(z)=F_0(0)e^{i\gamma z/2},\quad B_0(z)=B_0(0)e^{-i\gamma^*z/2},$$

$$|F_0(z)|^2=|B_0(z)|^2=|F_0(0)|^2e^{-\gamma_i z}, \tag{17}$$

where $\gamma\equiv\gamma_r+i\gamma_i=k_0n_0^3rE_{sc}/2$ is the coupling constant of the photorefractive crystal, which can easily be obtained from experiment by using Eqs. (17). Then the z-dependence of the characteristic relaxation time for the space-charge field has the form

$$t_d(z)=t_d(0)e^{\gamma_i z}. \tag{18}$$

Equations (4), (6), (8), (9), and (15)–(18), can be used to obtain a closed system of equations for the weak-beam amplitudes. For subsequent calculations it is convenient to write this system in matrix form:

$$\mathbf{J}\partial_t\mathbf{\Psi}_k=\mathscr{L}\mathbf{\Psi}_k+\sum_{\mathbf{k}_1+\mathbf{k}_2=\mathbf{k}}\boldsymbol{\eta}(\mathbf{\Psi}_{k_1},\mathbf{\Psi}_{k_2})+\sum_{\mathbf{k}_1+\mathbf{k}_2+\mathbf{k}_3=\mathbf{k}}\mathbf{\Theta}(\mathbf{\Psi}_{k_1},\mathbf{\Psi}_{k_2},\mathbf{\Psi}_{k_3}), \tag{19}$$

where

$$\mathbf{\Psi}_k=(F_k,F^*_{-k},B_k,B^*_{-k},E_{2k_0,k},E_{-2k_0,k}) \tag{20}$$

is a six-dimensional vector,

$$\mathbf{J}=e^{\gamma_i z}\begin{pmatrix}\mathbf{0}&&\\&\mathbf{0}&\\&&\mathbf{1}\end{pmatrix} \tag{21}$$

is a diagonal 6×6 matrix, and $\mathbf{0}$, $\mathbf{1}$ are respectively the zero and unit 2×2 matrices. The linear operator $\mathscr{L}$ has the form

$$\mathscr{L}=-\mathbf{N}i\partial_z-\mathbf{K}k_d+\frac{1}{2}\times\begin{pmatrix}\gamma&0&-\gamma&0&-\gamma&0\\0&-\gamma^*&0&\gamma^*&0&\gamma^*\\\gamma^*&0&-\gamma^*&0&0&\gamma^*\\0&-\gamma&0&\gamma&-\gamma&0\\1&-1&-1&1&-2&0\\-1&1&1&-1&0&-2\end{pmatrix}, \tag{22}$$

where

$$\mathbf{N}=\begin{pmatrix}\mathbf{1}&&\\&\mathbf{1}&\\&&\mathbf{0}\end{pmatrix},\quad \mathbf{K}=\begin{pmatrix}-\boldsymbol{\sigma}_3&&\\&\boldsymbol{\sigma}_3&\\&&\mathbf{0}\end{pmatrix}$$

are diagonal 6×6 matrices, σ_3 is a Pauli matrix, $k_d=k^2/2k_0n_0$, and the time t has been made dimensionless by dividing it by the characteristic relaxation time of the field E at the front face of the crystal: $t/t_d(0)\to t$.

The quadratic nonlinearity in Eq. (19) is written in the form of a vector $\boldsymbol{\eta}$ that depends on the two arguments $\mathbf{\Psi}_{k_1}$ and $\mathbf{\Psi}_{k_2}$:

$$\boldsymbol{\eta}(\mathbf{\Psi}_{k_1},\mathbf{\Psi}_{k_2})=\begin{pmatrix}-\frac{\gamma}{2}E_{2k_0,k_1}B_{k_2}\\\frac{\gamma^*}{2}E_{-2k_0,k_1}B^*_{-k_2}\\\frac{\gamma^*}{2}E_{-2k_0,k_1}F_{k_2}\\-\frac{\gamma}{2}E_{2k_0,k_1}F^*_{-k_2}\\-\frac{1}{2}F_{k_1}F^*_{-k_2}-\frac{1}{2}B_{k_1}B^*_{-k_2}+F_{k_1}B^*_{-k_2}-\frac{1}{2}E_{2k_0,k_1}(F_{k_2}+F^*_{-k_2}+B_{k_2}+B^*_{-k_2})\\-\frac{1}{2}F_{k_1}F^*_{-k_2}-\frac{1}{2}B_{k_1}B^*_{-k_2}+B_{k_1}F^*_{-k_2}-\frac{1}{2}E_{-2k_0,k_1}(F_{k_2}+F^*_{-k_2}+B_{k_2}+B^*_{-k_2})\end{pmatrix}, \tag{23}$$

while the cubic nonlinearity vector $\mathbf{\Theta}$ depends on three arguments:

$$\mathbf{\Theta}(\mathbf{\Psi}_{k_1},\mathbf{\Psi}_{k_2},\mathbf{\Psi}_{k_3})=\begin{pmatrix}0\\0\\0\\0\\-\frac{1}{2}E_{2k_0,k_1}(F_{k_2}F^*_{-k_3}+B_{k_2}B^*_{-k_3})\\-\frac{1}{2}E_{-2k_0,k_1}(F_{k_2}F^*_{-k_3}+B_{k_2}B^*_{-k_3})\end{pmatrix}, \tag{24}$$

Equations (19) must be supplemented by boundary conditions. In particular, at the back face of the crystal the sideband beams B_k acquire an additional phase due to reflection of the F_k beam from the feedback mirror. In order to obtain this phase shift, let us find the difference in the optical paths of two parallel rays 1 and 2 incident at an angle θ' on the back face AC of the crystal (see Fig. 1). The optical path difference $\Delta_{1,2}$ will then have the form

$$\Delta_{1,2}=l_{AB}+l_{BC}-n_0l_{CD}+\lambda/2,$$

where

$$l_{AB}=l_{BC}=L/\cos\,\theta,\quad l_{CD}=2L\,\tan\,\theta\,\sin\,\theta',$$

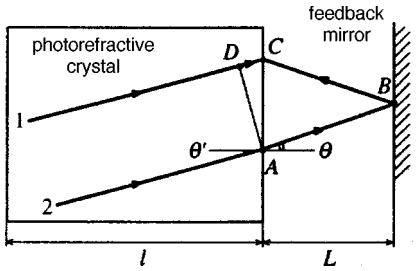

FIG. 1. Segment *DA* is perpendicular to the direction of propagation of rays *1* and *2* within the photorefractive crystal.

$$\sin\theta/\sin\theta' = n_0,$$

L is the distance between the feedback mirror and the back face of the crystal, and λ is the wavelength of the light in vacuum. Subtracting the path difference of the pump beams $2L+\lambda/2$ from the optical path difference $\Delta_{1,2}$, we obtain the required phase shift ϕ (in the small-angle approximation $\theta \ll 1$):

$$\phi = 2L(\cos\theta - 1)k_0 \simeq -2k_d n_0 L,$$

while the boundary conditions for the sideband waves have the form

$$\begin{aligned} &F_k(0) = F^*_{-k}(0) = 0,\\ &B_k(l) = F_k(l)\exp(-2ik_d n_0 L),\\ &B^*_{-k}(l) = F^*_{-k}(l)\exp(2ik_d n_0 L), \end{aligned} \tag{25}$$

where l is the length of the crystal along the z axis. Note that the signs of the exponents in (25) are reversed compared to Ref. 12. This discrepancy is obviously due to a typographical error in Ref. 12, since subsequent expressions in this paper are correct.

Thus, the problem of describing the evolution of sideband waves reduces to a boundary value problem for the system of equations (19) with boundary conditions (25). A characteristic feature of the photorefractive nonlinearity is the fact that the right side of Eq. (19), and consequently the stationary solutions of the boundary-value problem (19), (25), are independent of the pump intensity I_Σ. The pump intensity determines only the overall normalization of the optical intensities and the characteristic time t_d for setting up the stationary solutions.

3. LINEAR INSTABILITY THEORY

As a first step, let us study the evolution of sideband waves in the linear approximation. The system (19) is linearized by discarding the nonlinear (in $\mathbf{\Psi}_k$) terms $\boldsymbol{\eta}$, $\boldsymbol{\Theta}$. If we assume that the time dependence of $\mathbf{\Psi}_k$ has the form $\mathbf{\Psi}_k \propto \exp(\nu_k t)$, we obtain a linear boundary value problem for the complex eigenvalues ν_k:

$$\mathscr{L}\mathbf{\Psi}_k = \nu_k \mathbf{J}\mathbf{\Psi}_k. \tag{26}$$

Solution of this boundary value problem in the general case presents considerable difficulty, because Eq. (26) is a system of ordinary differential equations (in the coordinate z) with nonconstant coefficients. The linear boundary value problem can be solved in two special cases where the system reduces to a system of ordinary differential equations with constant coefficients. The first is the case where the coupling constant $\gamma = \gamma_r$ is real (a medium with a local photorefractive response). Then $|F_0(z)|^2 = |B_0(z)|^2 = \text{const}$. This case was investigated in Ref. 13 under the additional condition $\mathrm{Re}\,\nu_k = 0$, i.e., the instability threshold was found. However, the coupling constant can be treated approximately as a real number only in photorefractive crystals like $LiNbO_3$ and $LiTaO_3$, and no one has experimentally observed the formation of hexagons in these crystals to date. In the crystals $KNbO_3$ and $BaTiO_3$ discussed in this paper, the constant is unequivocally complex; in fact, we have $\gamma \simeq i\gamma_i$ (indicating a nonlocal photorefractive response).[10,15] In the second case, the coupling constant γ is an arbitrary complex quantity, but it is assumed that the reflection coefficient from the feedback mirror is exactly equal to 1, i.e., $R=1$ (reflection from the crystal faces is neglected as before), and hence $|F_0(z)|^2 = |B_0(z)|^2$. It is also necessary to assume that $\nu_k = 0$. This implies that the boundary value problem is solved at the instability threshold $\mathrm{Re}\,\nu_k = 0$, and that this instability is aperiodic, so that $\mathrm{Im}\,\nu_k = 0$, i.e., the frequency detuning between pump beams and sideband beams vanishes. If it were the case that the detuning satisfied $\mathrm{Im}\,\nu_k \neq 0$, a moving optical pattern would be observed in the experiment. However, the experiments of Refs. 8 and 12 showed that the optical pattern is motionless; therefore, the assumption $\mathrm{Im}\,\nu_k = 0$ appears to be fully justified. The boundary value problem with $R=1$, $\nu_k = 0$ was solved in Ref. 12. In this case the system (26) takes the form

$$\begin{aligned} &\left(\frac{d}{dz} + ik_d\right)F_k = -\frac{i\gamma}{4}(F_k + F^*_{-k} - B_k - B^*_{-k}),\\ &\left(\frac{d}{dz} - ik_d\right)F^*_{-k} = \frac{i\gamma^*}{4}(F_k + F^*_{-k} - B_k - B^*_{-k}),\\ &\left(\frac{d}{dz} - ik_d\right)B_k = -\frac{i\gamma^*}{4}(F_k + F^*_{-k} - B_k - B^*_{-k}),\\ &\left(\frac{d}{dz} + ik_d\right)B^*_{-k} = \frac{i\gamma}{4}(F_k + F^*_{-k} - B_k - B^*_{-k}),\\ &E_{2k_0,k} = \frac{1}{2}(F_k - F^*_{-k} - B_k + B^*_{-k}),\\ &E_{-2k_0,k} = -\frac{1}{2}(F_k - F^*_{-k} - B_k + B^*_{-k}), \end{aligned} \tag{27}$$

where the space-charge field amplitudes were eliminated from the first four equations by using the last two equations of the system. The solution to the system (27) combined with the boundary conditions (25) leads to the threshold condition for appearance of the instability, which exactly coincides with the results of Ref. 12

$$\cos(wl)\cos(k_d l) + \frac{\gamma_i}{2w}\sin(wl)\cos[k_d(l + 2n_0 L)]$$

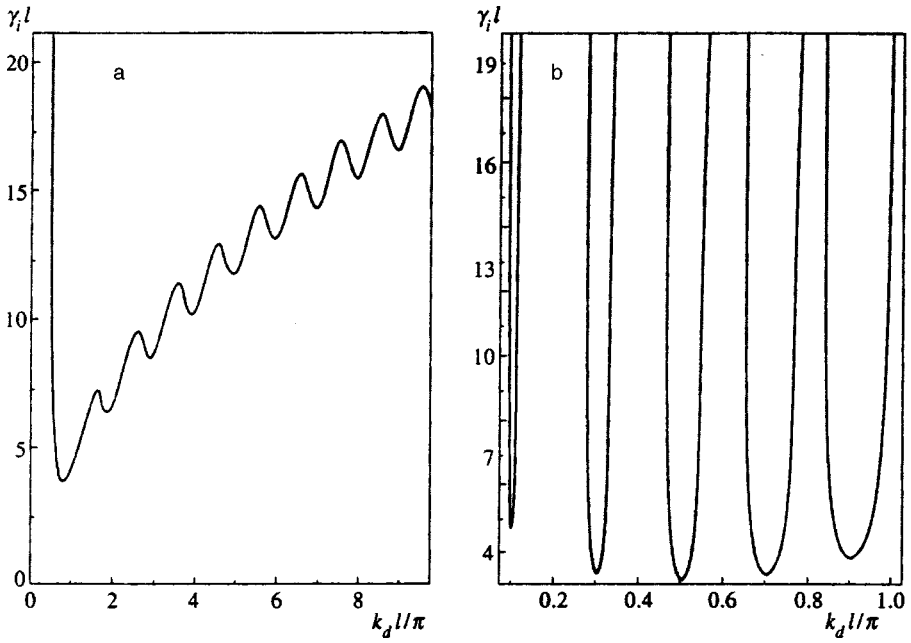

FIG. 2. Threshold dependence of $\gamma_i l$ on $k_d l$ for $L=0$ (a) and $n_0 L/l=4.44$ (b).

$$+\frac{\gamma_r+2k_d}{2w}\sin(wl)\sin(k_d l)-\frac{\gamma_r}{2w}\sin(wl)$$

$$\times\sin[k_d(l+2n_0L)]=0, \tag{28}$$

where $w=\sqrt{k_d^2+\gamma_r k_d-\gamma_i^2/4}$. As we have already noted, the coupling constant satisfies $\gamma\simeq i\gamma_i$ in the $KNbO_3$ and $BaTiO_3$ crystals to high accuracy, i.e., is pure imaginary. Therefore, in what follows we will set $\gamma=i\gamma_i$, and then obtain the threshold function $\gamma_i(k_d l)$ from Eq. (28) for each value of the distance to the feedback mirror L. This function consists of a sequence of minima. Figure 2 shows special cases of the threshold curves $\gamma_i(k_d l)$ for $L=0$ and $n_0 L/l=4.44$; in the second case, the dependence of $\gamma_i l$ on $k_d l$ is so steep that only those parts of the threshold curve near the minima could be plotted. The region of instability lies above the threshold curve $\gamma_i(k_d l)$. As L changes, the position of the minima changes; however, the number of minima and their relative spacings remain unchanged, which allows us to label them in order of increasing $k_d l$ as 1,2,3,⋯, etc. In what follows a positive integer m is used to label each minimum. For $n_0 L/l<1.43\cdots$, the first minimum $m=1$ is the deepest, while as L increases the second minimum becomes deepest, then the third, etc., in succession. Figure 3 shows the L-dependence of $\gamma_i^{\min} l$ and $k_d^{\min} l$ corresponding to these minima. There is only one set of values of the parameter L for which $\gamma_i^{\min} l$ and $k_d^{\min} l$ can be found analytically, namely

$$n_0 L/l=-3/2+2m, \quad \gamma_i^{\min} l=\pi, \quad k_d^{\min} l=\pi/2, \tag{29}$$

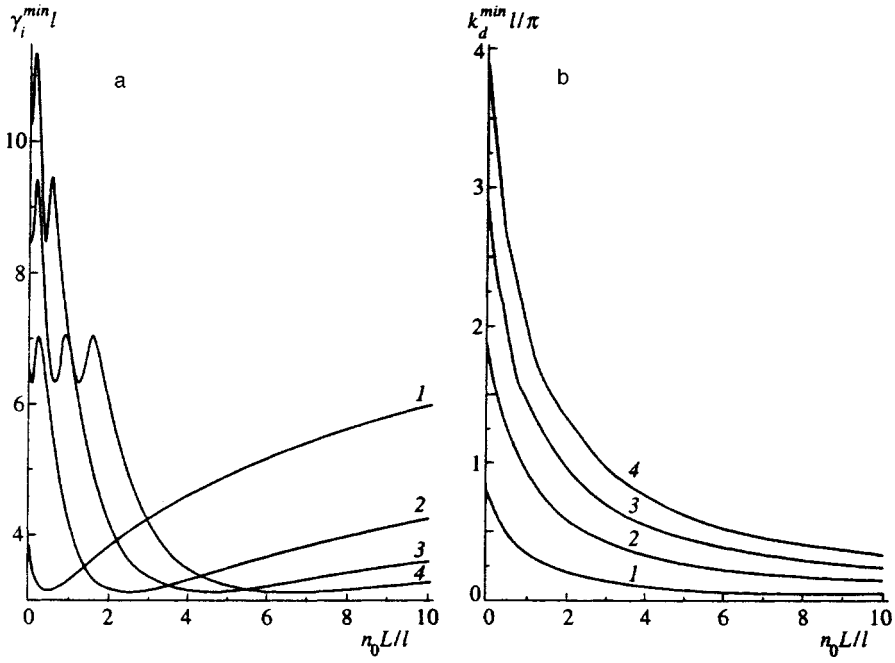

FIG. 3. Dependence of $\gamma_i^{\min} l$ (a) and $k_d^{\min} l$ (b) on the dimensionless distance to the feedback mirror $n_0 L/l$.

It is clear from Fig. 3a that at these values of L the minimum value $\gamma_i^{\min} l=\pi$ is reached as a function of L. It is important to note that for $n_0 L/l \gtrsim -3/2+2m$ the position of the mth minimum is given with high accuracy by the relation

$$k_d(l+2n_0L)=(2m-1)\pi \tag{30}$$

(which is an identity when Eq. (29) holds). The limiting case of this relation for $2n_0L/l \gg 1$, $m=1$ has been seen in experiments.[8] Actually, condition (30) implies that we are choosing that phase shift in Eq. (25) between sideband beams propagating in opposite directions along the z axis for which these beams interact most efficiently. In order to understand the physical meaning of Eq. (30), let us investigate the dependence of the space-charge field amplitude $E_{2k_0,k}$ on the z coordinate. From Eqs. (27) and (25) we find

$$\begin{aligned} F_k+B_{-k}^*&=\exp[-ik_d(z-l)][F_k(l)\\ &\quad+\exp(2ik_dn_0L)F_{-k}^*(l)],\\ F_{-k}^*+B_k&=\exp[ik_d(z-l)]\\ &\quad\times[\exp(-2ik_dn_0L)F_k(l)+F_{-k}^*(l)]. \end{aligned} \tag{31}$$

Then from Eq. (27) it follows that

$$\begin{aligned} E_{2k_0,k}=i\,\sin[k_d(l-z+n_0L)][&\exp(-ik_dn_0L)F_k(l)\\ &+\exp(ik_dn_0L)F_{-k}^*(l)]. \end{aligned} \tag{32}$$

Physical considerations suggest that the lowest instability threshold corresponds to the most effective interaction between sideband waves mediated by the space-charge field $E_{2k_0,k}$. According to Eq. (32), the amplitude of this field is sinusoidal, and thus on the average the magnitude of the field amplitude will be a maximum within the crystal when the peak of the sinusoid is located at the center of the crystal $z=l/2$, from which we obtain $k_d(l/2+n_0L)=(m-1/2)\pi$, where m is a whole number, which exactly coincides with Eq. (30). Numerical calculations actually confirm that when $n_0L/l \gtrsim -3/2+2m$ holds the maximum of the amplitude $E_{2k_0,k}$ coincides to good accuracy with the center of the crystal, and that for values of k_d away from the threshold minimum $k_d=k_d^{\min}$ the maximum of this amplitude moves away from the crystal center. Nevertheless, the physical justification presented above is somewhat qualitative, because in addition to the interaction of sideband beams via the field $E_{2k_0,k}$ there is also a contribution associated with diffraction of the sideband beams by the space-charge field of the pump beams E_{2k_0}, as is apparent from the linear part of the system Eq. (19). This contribution does not allow such a simple interpretation; however, our success in explaining Eq. (30) is reason to hope that the overall physical justification is correct.

Let us now allow γ_i to exceed threshold somewhat: $0<h=(\gamma_i-\gamma_i^{\min})/\gamma_i^{\min} \ll 1$, where $\gamma_i^{\min}$ corresponds to the deepest minimum for a given value of L. Near threshold the instability growth rate can be written in the form

$$\nu_k=\nu_0-(k_d-k_d^{\min})^2 f,$$

where ν_0 is the maximum instability growth rate, $|k_d-k_d^{\min}|/k_d^{\min} \ll 1$, and $f>0$ is a constant. Because the linear boundary value problem cannot be solved analytically for $\nu_k \neq 0$, the values of ν_0 and f remain unknown. However, it will be clear from what follows that these values themselves are not important for the existence of an explosive three-wave instability. Furthermore, although ν_0 gives a correction to the hexagon amplitudes, near threshold we have $\nu_0 \to 0$ and so this correction is negligibly small. Since the value of ν_0 is positive above threshold, in the linear approximation the amplitudes F_k and B_k will grow exponentially with time until the three-wave nonlinearity becomes important. For small values of the ''supercriticality'' h, the gain of the instability is positive only within a narrow ring $|\mathbf{k}| \simeq \sqrt{2k_d^{\min}k_0n_0}$, so that when sideband waves are excited in this ring, the magnitudes of their transverse wave vectors $|\mathbf{k}|$ can be treated as practically constant.

In addition to the threshold condition (28), the linear boundary value problem Eqs. (27) and (25) allows us to find the six-dimensional eigenvector Eq. (20) $\boldsymbol{\psi}_k^{(0)}$ of this problem at the instability threshold. The zero superscript indicates that all quantities are calculated at the threshold point, and the lower case symbol $\boldsymbol{\psi}_k$ is used in place of the upper-case symbol $\boldsymbol{\Psi}_k$ to emphasize that the latter is a solution to the nonlinear boundary value problem, while the former is a solution to its linear portion only.

Let us briefly describe the procedure for finding $\boldsymbol{\psi}_k^{(0)}$: the general solution to the system of four ordinary differential equations (27) can be written in the form of a sum of four independent solutions with arbitrary coefficients $\mathbf{c}=(c_1,c_2,c_3,c_4)$. The values of these coefficients are determined from boundary conditions (25), which reduce to a homogenous system of linear equations for $\mathbf{c}$. The condition that the system be solvable is that its determinant vanish, which leads to the threshold condition (28), from which we find a solution $\mathbf{c}$ of the homogenous system of linear equations defined up to an arbitrary factor. Therefore, the eigenvector $\boldsymbol{\psi}_k^{(0)}$ is also determined up to an arbitrary factor. In particular, for $n_0L/l=-3/2+2m$, $\gamma_i^{\min} l=\pi$, $k_d^{\min} l=\pi/2$ we obtain

$$\boldsymbol{\psi}_k^{(0)} = \begin{pmatrix} -i\,\exp\left[-i\,\frac{\pi}{2}\left(\frac{z}{l}-\frac{1}{2}\right)\right]+\exp\left(\frac{3}{4}\,i\pi\right)\exp\left(\frac{\pi z}{2l}\right)\\ i\,\exp\left[\frac{i}{2}\,\pi\left(\frac{z}{l}-\frac{1}{2}\right)\right]+\exp\left(-\frac{3}{4}\,i\pi\right)\exp\left(\frac{\pi z}{2l}\right)\\ i\,\exp\left[\frac{i}{2}\,\pi\left(\frac{z}{l}-\frac{1}{2}\right)\right]+\exp\left(\frac{1}{4}\,i\pi\right)\exp\left(\frac{\pi z}{2l}\right)\\ -i\,\exp\left[-\frac{i}{2}\,\pi\left(\frac{z}{l}-\frac{1}{2}\right)\right]+\exp\left(-\frac{1}{4}\,i\pi\right)\exp\left(\frac{\pi z}{2l}\right)\\ -i2\cos\left[\frac{\pi}{2}\left(\frac{z}{l}-\frac{1}{2}\right)\right]\\ i2\cos\left[\frac{\pi}{2}\left(\frac{z}{l}-\frac{1}{2}\right)\right] \end{pmatrix}. \tag{33}$$

For arbitrary values of L the explicit form of this vector

is very complicated and will not be given here. For each specific value of the parameters $\gamma_i^{\min} l$, $k_d^{\min} l$, L the eigenvector $\boldsymbol{\psi}_k^{(0)}$ was found using the program Mathematica 2.2.

In order to find the three- and four-wave interactions it is also necessary to solve a linear boundary value problem, which is the Hermitian conjugate of the linear portion of the boundary value problem Eqs. (19) and (25) with respect to the scalar product

$$\langle \boldsymbol{\psi}_k^c | \boldsymbol{\psi}_k \rangle = \int_0^l dz (\psi_k^{c\,i})^* \psi_k^i. \tag{34}$$

Here repetition of the label i implies summation from 1 to 6, and $\boldsymbol{\psi}_k^c$ is an eigenvector of this Hermitian-conjugate problem that satisfies the system of equations

$$\mathscr{L}^+ \boldsymbol{\psi}_k^c = 0 \tag{35}$$

at the instability threshold. The operator $\mathscr{L}^+ \equiv (\mathscr{L}^T)^*$ is the Hermitian conjugate of (22), and the following boundary conditions are imposed on the components of the vector $\boldsymbol{\psi}_k^c$:

$$\begin{aligned} &B_k^c(0) = B_{-k}^{c*}(0) = 0, \\ &B_k^c(l) = -F_k^c(l) \exp(-2ik_d n_0 L), \\ &B_{-k}^{c*}(l) = -F_{-k}^{c*}(l) \exp(2ik_d n_0 L), \end{aligned} \tag{36}$$

obtained by integrating the Hermitian operator id/dz by parts.

The solution of the Hermitian-conjugate boundary value problem (35), (36) is analogous to the solution of the original boundary value problem (27), (25), and the threshold condition for the Hermitian-conjugate problem coincides with the threshold condition (28) for the direct problem. The eigenvector for the conjugate problem takes the following form when $n_0 L/l = -3/2 + 2m$, $\gamma_i^{\min} l = \pi$, $k_d^{\min} l = \pi/2$:

$$\boldsymbol{\psi}_k^{c(0)} = \begin{pmatrix} \exp\left[-i\frac{\pi}{2}\left(\frac{z}{l}-\frac{1}{2}\right)\right] + \exp\left(i\frac{\pi}{4}-\frac{\pi z}{2l}\right) \\ \exp\left[i\frac{\pi}{2}\left(\frac{z}{l}-\frac{1}{2}\right)\right] + \exp\left(-i\frac{\pi}{4}-\frac{\pi z}{2l}\right) \\ \exp\left[i\frac{\pi}{2}\left(\frac{z}{l}-\frac{1}{2}\right)\right] + \exp\left(i\frac{3\pi}{4}-\frac{\pi z}{2l}\right) \\ \exp\left[-i\frac{\pi}{2}\left(\frac{z}{l}-\frac{1}{2}\right)\right] + \exp\left(-i\frac{3\pi}{4}-\frac{\pi z}{2l}\right) \\ i\pi \exp\left[-i\frac{\pi}{2}\left(\frac{z}{l}-\frac{1}{2}\right)\right] \\ i\pi \exp\left[i\frac{\pi}{2}\left(\frac{z}{l}-\frac{1}{2}\right)\right] \end{pmatrix}. \tag{37}$$

4. THREE-WAVE INTERACTION OF SIDEBAND WAVES

The investigation of three- and four-wave interactions given here will follow several ideas taken from Refs. 18 and 19, in which the generation of hexagonal cells was discussed at the surface of a liquid dielectric in an external electric field (Refs. 18) and under conditions of weakly supercritical convection (Refs. 19).

Let us expand the general solution $\boldsymbol{\Psi}_k$ of the nonlinear boundary value problem (19), (25) within the ring $|\mathbf{k}| \simeq \sqrt{2k_d^{\min} k_0 n_0}$ in eigenvectors $\boldsymbol{\psi}_{k,n}$ of the linear boundary value problem (27), (25):

$$\boldsymbol{\Psi}_k = \sum_n \boldsymbol{\psi}_{k,n} A_{k,n}(t), \quad A_{-k} = A_k^*, \tag{38}$$

where the letter n labels the eigenmode of the linear problem for a given value of the wave vector k.

Substituting this expression into the nonlinear system (19) and taking the scalar product of the latter (as in Eq. (34)) with the eigenvector $\boldsymbol{\psi}_k^c$ of the conjugate linear problem leads to the following equation, which is accurate up to quadratic nonlinearities:

$$\frac{\partial A_{k,n}}{\partial t} = \nu_{k,n} A_{k,n} + \frac{1}{2} \sum_{n_1,n_2} \sum_{\mathbf{k}_1+\mathbf{k}_2=\mathbf{k}} U_{k_1,k_2,k}^{n_1,n_2,n} A_{k_1,n_1} A_{k_2,n_2}, \tag{39}$$

where $U_{k_1,k_2,k}^{n_1,n_2,n}$ is the matrix element of the three-wave interaction.

Since for small values of the supercritical parameter $0 < h = (\gamma_i - \gamma_i^{\min})/\gamma_i^{\min} \ll 1$ sideband waves are excited only in the narrow ring $|\mathbf{k}| \simeq \sqrt{2k_d^{\min} k_0 n_0}$ corresponding to the mode with maximum gain and label $n=0$, while the other modes have negative gain, to find the matrix element we need only calculate it at the instability threshold $k_d = k_d^{\min}$, $\gamma = i\gamma_i^{\min}$, $\boldsymbol{\psi}_{k,n} = \boldsymbol{\psi}_k^{(0)}$, $\boldsymbol{\psi}_{k,n}^c = \boldsymbol{\psi}_k^{c(0)}$ for $n=0$. Therefore, in what follows the label n will be omitted. Furthermore, the condition $\mathbf{k}_1 + \mathbf{k}_2 = \mathbf{k}$ implies that only vectors that make angles of $\pi/3$ with each other will participate in the three-wave interaction.

As a result, we obtain from Eq. (19)

$$U_{k_1,k_2,k} \equiv U = 2 \frac{\langle \boldsymbol{\psi}_k^c | \boldsymbol{\eta}_0 \rangle}{\langle \boldsymbol{\psi}_k^c | \mathbf{J} \boldsymbol{\psi}_k \rangle}, \tag{40}$$

where $\mathbf{J}$ and $\boldsymbol{\eta}$ are defined in Eqs. (21) and (23). The zero label in $\boldsymbol{\eta}_0$ indicates that its arguments are evaluated at the instability threshold, $\boldsymbol{\eta}_0 = \boldsymbol{\eta}(\boldsymbol{\psi}_k^{(0)}, \boldsymbol{\psi}_k^{(0)})$, and Eq. (39) reduces to Eq. (3).

For each specific set of values of the parameters $\gamma_i^{\min} l$, $k_d^{\min} l$, L the matrix element U was found using the program Mathematica 2.2. In the first step, the eigenvectors $\boldsymbol{\psi}_k^{(0)}$, $\boldsymbol{\psi}_k^{c(0)}$ were calculated for the direct and conjugate linear problems, and then the value of U was obtained by integration in Eq. (40). For the special cases $n_0 L/l = -3/2 + 2m$, $\gamma_i^{\min} l = \pi$, $k_d^{\min} l = \pi/2$ an analytic expression for the matrix element follows from Eqs. (33) and (37):

$$U = -\frac{2\sqrt{2}}{5} \frac{1 + 2e^{\pi}}{\cosh(\pi/2)}. \tag{41}$$

Figure 4 shows how the matrix element U for the three-wave interaction at the instability threshold depends on the distance L between the back face of the crystal and the feedback mirror (for the first minimum $m=1$ of the threshold curve $\gamma_i^{\min}(L)$), calculated from Eqs. (40) and (23), where the functions $\gamma_i^{\min}(L)$ and $k_d^{\min}(L)$ are given in Fig. 3. In this case, it was assumed that the coupling constant γ is pure imaginary,

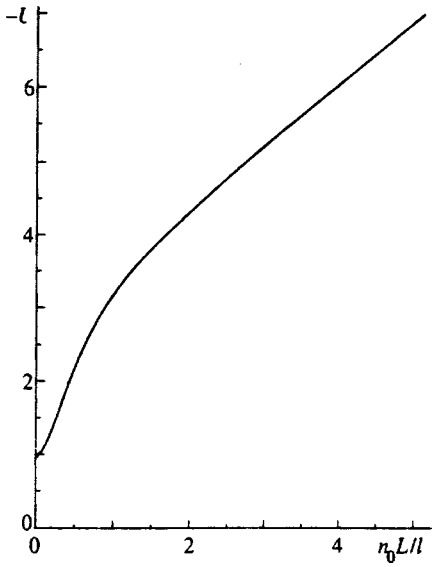

FIG. 4. Dependence of the three-wave interaction matrix element U on n_0L/l.

which is true for $KNbO_3$ and $BaTiO_3$ to high accuracy. The fact that U is a purely real quantity is very important for investigating the explosive instability.

5. FOUR-WAVE INTERACTION OF SIDEBAND WAVES

The explosive three-wave instability can be saturated by nonlinearities of fourth and higher orders. Those light beams whose wave vectors lie in the narrow ring near the instability threshold $|\mathbf{k}| \simeq \sqrt{2k_d^{\min}k_0n_0} \equiv k_{0\perp}$ will be referred to as ''fundamental'' spatial harmonics. The quadratic nonlinearities, represented by the vector $\boldsymbol{\eta}$ in the fundamental system of equations (19) and written out in Eq. (23), give rise to all possible sum and difference harmonics arising from the three-wave interaction $\mathbf{k}=\mathbf{k}_1+\mathbf{k}_2$, $|\mathbf{k}_{1,2}|=k_{0\perp}$.

Equations for the harmonics $\mathbf{k}=\mathbf{k}_1+\mathbf{k}_2$, $|\mathbf{k}_{1,2}|=k_{0\perp}$ follow from Eqs. (19) and (25), where $k_d=k^2/2k_0n_0$. The summation in the quadratic nonlinearities runs over fundamental harmonics at the instability threshold $\boldsymbol{\psi}_k=\boldsymbol{\psi}_k^{(0)}$, and time derivatives and cubic nonlinearities are neglected because the corrections they produce are of higher order (fifth order and higher). Thus, when the amplitudes of the fundamental harmonics are specified the boundary-value problem for combination harmonics reduces to the solution of a linear system of ordinary differential equations with constant coefficients and an inhomogeneous part determined by the amplitudes of the fundamental harmonics. The boundary conditions for this system are, as before, given by Eqs. (25). Solution of this system presents no fundamental difficulties; however, explicit expressions for the combination harmonics are not given here because they are extremely involved. It is important to note that these harmonics are second order in the amplitudes of the sideband waves, and therefore they contribute to the four-wave processes via the interaction with the fundamental harmonics. Furthermore, the four-wave interaction contains a contribution from the intrinsic process $2\rightarrow 2$ due to interaction of the fundamental spatial harmonics that arise from the cubic nonlinearities in the fifth and sixth equations of the system (19).

Thus, the general solution $\boldsymbol{\Psi}_k^{\mathrm{tot}}$ of the nonlinear boundary value problem (19), (25) can be cast in the form

$$\boldsymbol{\Psi}_k^{\mathrm{tot}}=\boldsymbol{\Psi}_k+\delta\boldsymbol{\Psi}_k, \tag{42}$$

where $\boldsymbol{\Psi}_k$ is an expansion of (38) in fundamental harmonics and

$$\delta\boldsymbol{\Psi}_k=\sum_{\mathbf{k}_1+\mathbf{k}_2=\mathbf{k}} A_{k_1}A_{k_2}\delta\boldsymbol{\Psi}_k$$

is an expansion in combination harmonics. The vectors $\mathbf{k}_1$ and $\mathbf{k}_2$ lie at the instability threshold $|\mathbf{k}_1|=|\mathbf{k}_2|=k_{0\perp}$.

Substituting Eqs. (42) and (43) into the nonlinear system (19) and taking the scalar product of this system according to (34) with the vector $\boldsymbol{\psi}_k^c$ of the conjugate linear problem (27) leads to the following equation, which is accurate to within cubic nonlinearities:

$$\begin{aligned}\frac{\partial A_k}{\partial t}=\nu_kA_k+\frac{U}{2}\sum_{\mathbf{k}_1+\mathbf{k}_2=\mathbf{k}}A_{k_1}A_{k_2}-\sum_{\mathbf{k}_1+\mathbf{k}_2+\mathbf{k}_3=\mathbf{k}}\\ \times\{[-\langle\boldsymbol{\psi}_k^{c(0)}|\boldsymbol{\eta}(\boldsymbol{\psi}_{k_1}^{(0)},\delta\boldsymbol{\Psi}_{k_2+k_3})-\boldsymbol{\eta}(\delta\boldsymbol{\Psi}_{k_2+k_3},\boldsymbol{\psi}_{k_1}^{(0)})\rangle\\ -\langle\boldsymbol{\psi}_k^{c(0)}|\boldsymbol{\Theta}(\boldsymbol{\psi}_{k_1}^{(0)},\boldsymbol{\psi}_{k_2}^{(0)},\boldsymbol{\psi}_{k_3}^{(0)})\rangle]/\langle\boldsymbol{\psi}_k^{c(0)}|\mathbf{J}\boldsymbol{\psi}_k^{(0)}\rangle\}\\ \times A_{k_1}A_{k_2}A_{k_3},\end{aligned} \tag{43}$$

where $\mathbf{J}$, $\boldsymbol{\eta}$ are defined in Eqs. (21) and (23), and the summation runs over fundamental harmonics. Thus, we obtain Eq. (3). The matrix element of the four-wave interaction $T_{-kk_1k_2k_3}$ is found by symmetrizing the expression in curly brackets in Eq. (43). The matrix element $T_{-kk_1k_2k_3}$ depends only on the angles between the vectors $\mathbf{k}$, $\mathbf{k}_1$, $\mathbf{k}_2$, $\mathbf{k}_3$; therefore we will denote this matrix element by T_ϕ, where ϕ is the angle between the vectors $\mathbf{k}_1$ and $\mathbf{k}_2$.

In the special case where only six fundamental harmonics are excited with wave vectors $\mathbf{k}_1$, $\mathbf{k}_2$, $\mathbf{k}_3$, $\mathbf{k}_4$, $\mathbf{k}_5$, $\mathbf{k}_6$, forming a hexagon (Fig. 5), we obtain three types of combination harmonics: zero-order $|\mathbf{k}|\simeq 0$, second-order $|\mathbf{k}|\simeq 2k_{0\perp}$, and ''root-three''-order $|\mathbf{k}|\simeq\sqrt{3}k_{0\perp}$. These combination harmonics are generated by the interaction of pairs of fundamental harmonics at angles π, 0, and $\pi/3$, respectively. In Fig. 5 the second order harmonics are indicated by dotted lines, and the $\sqrt{3}$ harmonics are indicated by dashed lines. The zero-order harmonic renormalizes the pump beams, while the second-order and $\sqrt{3}$ harmonics form the vertices and centers of the faces of secondary hexagons, respectively. This is clear both from Fig. 5 and the experiments (see, e.g., Fig. 2 in Ref. 8). The interaction via second-order harmonics contributes to the matrix element T_0, while interaction via $\sqrt{3}$ harmonics contributes to $T_{\pi/3}$; interaction via zero-order harmonics contributes to both T_0 and $T_{\pi/3}$. The process $2\rightarrow 2$ also contributes to both T_0 and $T_{\pi/3}$.

Let us denote the amplitudes of the six fundamental harmonics $\mathbf{k}_1$, $\mathbf{k}_2$, $\mathbf{k}_3$, $\mathbf{k}_4$, $\mathbf{k}_5$, $\mathbf{k}_6$ by A_1, A_2, A_3, A_4, A_5, A_6. According to Eq. (38), only three amplitudes are indepen-

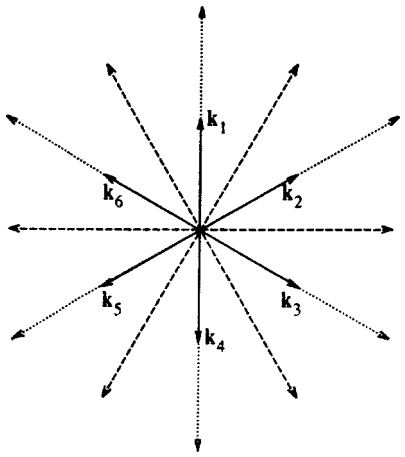

FIG. 5. The six vectors denoted by solid lines represent the fundamental harmonics. The ends of these vectors form the fundamental hexagon. The dotted lines denote the second-order harmonics, while the dashed lines are $\sqrt{3}$ harmonics. The second-order harmonics form the vertices of secondary hexagons, while the $\sqrt{3}$ harmonics are at the centers of their faces.

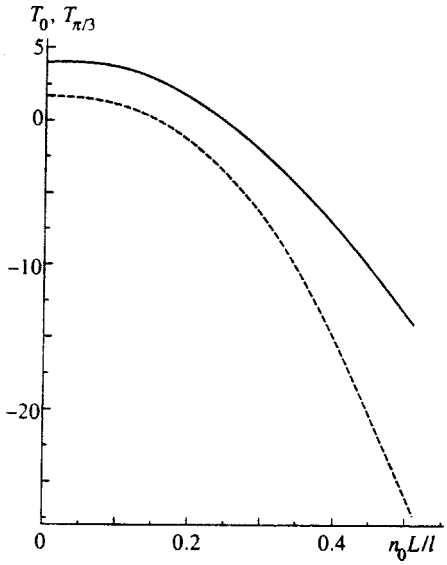

FIG. 6. Dependence of the matrix elements T_0, $T_{\pi/3}$ for four-wave interactions on n_0L/l; the solid curve is T_0, the dashed curve $T_{\pi/3}$.

dent: $A_4=A_1^*$, $A_5=A_2^*$, $A_6=A_3^*$, because $\mathbf{k}_4=-\mathbf{k}_1$, $\mathbf{k}_5=-\mathbf{k}_2$, $\mathbf{k}_6=-\mathbf{k}_3$. Then Eq, (3) can be rewritten in the form

$$\frac{\partial A_1}{\partial t}=\nu_0 A_1+UA_3^*A_5^*-\left[\frac{T_0}{2}|A_1|^2+T_{\pi/3}(|A_3|^2+|A_5|^2)\right]A_1,$$

$$\frac{\partial A_3}{\partial t}=\nu_0 A_3+UA_1^*A_5^*-\left[\frac{T_0}{2}|A_3|^2+T_{\pi/3}(|A_1|^2+|A_5|^2)\right]A_3, \tag{44}$$

$$\frac{\partial A_5}{\partial t}=\nu_0 A_5+UA_1^*A_3^*-\left[\frac{T_0}{2}|A_5|^2+T_{\pi/3}(|A_1|^2+|A_3|^2)\right]A_5.$$

Thus, the original boundary value problem (19), (25) reduces to a system of three amplitude equations.

The Mathematica 2.2 program was used to find the matrix elements T_0, $T_{\pi/3}$ for each specific value of the parameters $\gamma_i^{\min}l$, $k_d^{\min}l$, L, just as in the previous section where the three-wave interaction was discussed. Figure 6 shows the dependence of these matrix elements on the distance L between the back face of the crystal and the feedback mirror (for the first minimum $m=1$ of the threshold curve $\gamma_i^{\min}(L)$), calculated according to Eqs. (23) and (43), where $\gamma_i^{\min}(L)$, $k_d^{\min}(L)$ are given in Fig. 3. Just as for U, all of these matrix elements are found to be purely real quantities.

6. HEXAGON FORMATION DYNAMICS AND STABILITY

In the previous section, the problem of describing the evolution of hexagons was reduced to solution of the system (44) of three ordinary differential equations. When cubic nonlinearities are neglected, this system leads to an explosive instability. For equal and real amplitudes $A_1=A_3=A_5=\mathrm{Re}\,A_1$, we obtain (1) as a special case, whose corresponding solution (2) goes to infinity at finite time. In general, solutions to the system (44) (without cubic nonlinearities) can be expressed in terms of elliptic functions, and for arbitrary initial conditions (except for a set of measure zero) these solutions also exhibit singularities at finite times. It can be shown that in this limit the relative deviations $(|A_1|^2-|A_2|^2)/|A_1|^2$, $(|A_2|^2-|A_3|^2)/|A_2|^2$ go to zero, the total phase $\Phi=\mathrm{Arg}\,A_1+\mathrm{Arg}\,A_3+\mathrm{Arg}\,A_5$ goes to πn, where n is an integer, and each of the phases individually goes to a certain constant. Therefore, at later stages of evolution the system (44) reduces to the following equation for the intensity $I^2=|A_1|^2=|A_2|^2=|A_3|^2$:

$$\frac{1}{2}\frac{\partial I}{\partial t}=\nu_0 I+UI^{3/2}-\left(\frac{T_0}{2}+2T_{\pi/3}\right)I^2, \tag{45}$$

whose solution can be directly compared with experiment for small supercritical parameters when $\nu_0\to 0$.

Thus, the formation of hexagons admits the following physical picture. Due to fluctuations in the medium at time $t=0$, the amplitude A_1 is found to be nonzero for a certain value of wave vector $\mathbf{k}$ lying in the ring $|\mathbf{k}|\simeq\sqrt{2k_d^{\min}k_0n_0}$. The linear instability leads to an increase in $|A_1|$ until the nonlinear terms in Eq. (44) become important, as a result of which the amplitudes A_1, A_3, A_5 all begin to grow explosively at the same time, i.e., sideband waves are found to be excited with wave vectors $\mathbf{k}_1$, $\mathbf{k}_2$, $\mathbf{k}_3$, $\mathbf{k}_4$, $\mathbf{k}_5$, $\mathbf{k}_6$ forming a hexagon (see Fig. 5). The explosive growth of these amplitudes due to the three-wave interaction will continue until the four-wave nonlinearity comes into play. If in this case it turns out that the system parameters $\gamma_i^{\min}l$, $k_d^{\min}l$, n_0L/l are such that the total matrix element $T_0/2+2T_{\pi/3}$ is positive, then the four-wave nonlinearity can stabilize the instability; otherwise, the growth in intensity of the sideband waves con-

tinues and stabilization is achieved only via nonlinearities of higher order. In what follows, we will discuss the stability of stationary hexagonal solutions.

In experiment it has been well established[6,8] that initially two sideband waves are actually excited, with opposite signs of the transverse wave vectors. This exactly corresponds to the initial growth of amplitude A_1 for the ψ_k eigenmode Eq. (38), since this mode consists of sideband waves with transverse wave vectors $\pm\mathbf{k}$ (20). Then a rapid growth of hexagons is observed, and the intensities of all sideband waves are comparable.[8] In Ref. 8 the time dependence of the intensities of the sideband waves was measured. It is clear from Fig. 3 of Ref. 8 that after a short initial stage of exponential growth, the intensity follows a power-law increase that is characteristic of explosive nonlinearity, after which it is stabilized by higher-order nonlinearities. Evidence of this stabilization is the formation of secondary hexagons with low intensity (see Fig. 2 in Ref. 8) generated by second-order and $\sqrt{3}$ harmonics.

The stationary (hexagon) solution to Eq. (44) has the form

$$A_0=\frac{U}{4T_{\pi/3}+T_0}+\operatorname{sign}\ U\sqrt{\frac{2\nu_0}{4T_{\pi/3}+T_0}+\left(\frac{U}{4T_{\pi/3}+T_0}\right)^2}, \tag{46}$$

where $A_0=A_1=A_2=A_3$. This solution is characterized by a ''hard'' excitation regime, with an amplitude discontinuity at threshold (for $\nu_0=0$) given by

$$A_0=\frac{2U}{4T_{\pi/3}+T_0}.$$

The procedure for investigating the internal stability of the stationary solution (46) was analogous to that used in Ref. 19. This solution is stable when

$$-\frac{1}{2}\frac{U^2}{T_0+4T_{\pi/3}}<\nu_0<4\frac{T_0+T_{\pi/3}}{(2T_{\pi/3}-T_0)^2}U^2. \tag{47}$$

This result, when evaluated near the instability threshold where $\nu_0\to 0$, implies that $T_0+T_{\pi/3}>0$. Figure 7 shows the dependence of the hexagon intensity $I=A_0^2$ on n_0L/l in that range of the parameter L where the stability condition (47) holds. Outside this range, explosive growth of the hexagons can be stabilized only by higher-order wave processes.

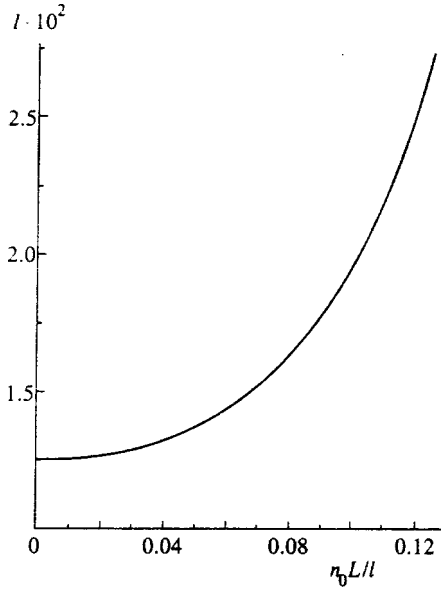

FIG. 7. Intensity I of the fundamental hexagon at the front face of the photorefractive crystal $z=0$ as a function of n_0L/l, which follows from the theory of four-wave interactions in the region where this theory is applicable. The intensity of the hexagon is normalized by the intensity of the pump at the front face of the crystal.

7. NUMERICAL EXPERIMENT

A numerical experiment was performed in order to verify the results of the analytic theory for hexagon generation described above. The goal of this experiment was to investigate the region of large values of $n_0L/l\gtrsim 0.1$, where saturation of the explosive instability is provided by higher-order wave processes (five-wave and higher). In the experiment the boundary value problem (19), (25) was solved numerically, taking into account a larger number of sum and difference harmonics than in the previous section. In order to estimate the number of higher-order harmonics required, and accordingly the order of the wave processes that must be included in order to definitely ensure saturation of the explosive instability, the following integral of the boundary value problem (19), (25) was used:

$$H=\sum_k\ (|F_k|^2-|B_k|^2)+[F_k+F_k^*-B_k-B_k^*]\Big|_{k=0}=0, \tag{48}$$

where the summation runs over all harmonics. The vanishing of this integral for all z at all times t physically expresses conservation of the energy of the optical field, since the dissipation of optical energy, which is small in a photorefractive crystal, has nowhere been taken into account in deriving the system (19), (25). In particular, at $z=0$ (i.e., at the front face of the crystal) the condition $H=0$ implies that the optical power of the pump beam incident on the crystal equals the total optical power of the beams that exit the crystal by its back face (recall that we have neglected reflection from the boundary and have set the reflection coefficient of the feedback mirror equal to unity). According to the boundary condition (25), we have $F_k|_{z=0}=0$ for all k; therefore it follows from Eq. (48) that when sideband waves form the pump is depleted, which is expressed in the growth of the zero-order harmonics $F_k|_{k=0}$, $B_k|_{k=0}$ which renormalize the pump beams. Thus, in the strongly nonlinear theory we must at a minimum take into account all processes in which zero harmonics interact with each other. It is not difficult to see that such processes give contributions up to eighth order in the equation for the fundamental harmonic. Therefore, in the numerical experiment all processes up to eight-wave inclusively were taken into account. In this case, it is necessary to include along with the harmonics 0, 1, 2, $\sqrt{3}$ listed above the harmonics $\sqrt{7}$, 3, $\sqrt{12}$, $\sqrt{13}$, 4 as well. (The ends of the

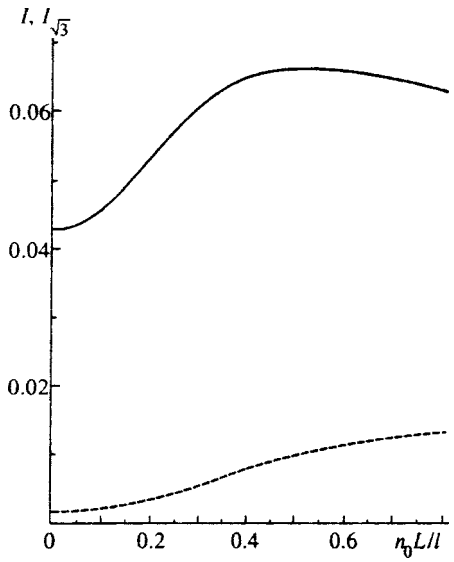

FIG. 8. Dependence of the intensity of the fundamental hexagon I (solid curve) and intensity of the $\sqrt{3}$ harmonic ($I_{\sqrt{3}}$ is dashed) on n_0L/l obtained from the numerical experiment. The normalization of the intensity is the same as in Fig. 7.

wave vectors of harmonics 3, $\sqrt{12}$, 4 form the vertices of hexagons, while the ends of the wave vectors of harmonics $\sqrt{7}$, $\sqrt{13}$ form regular dodecagons).

At each time t the boundary value problem (19), (25) was solved by Newton's method. At each step of this method, values of the amplitude $B_k|_{z=0}$ were specified at the front face of the crystal for all the harmonics. Then the amplitudes $F_k|_{z=l}$, $B_k|_{z=l}$ at the back face of the crystal were found by integrating the first four ordinary differential equations of the system (19) using the fourth-order Runge-Kutta method in the coordinate z. The error used in Newton's method was given by the accuracy with which the boundary condition (25) was satisfied at the back face of the crystal. The time dependence was determined by integrating the space charge field amplitudes $E_{\pm 2k_0,k}$ using a predictor-corrector method (the fifth and sixth equations of the system (19)).

The results of the numerical experiment are shown in Fig. 8 in the form of plots of the intensities of the fundamental harmonic and $\sqrt{3}$ harmonic versus the distance to the feedback mirror for $0 \leqslant n_0L/l \leqslant 0.85$. In the region $0 \leqslant n_0L/l \lesssim 0.1$, the intensity of the fundamental harmonic has a minimum, which is in agreement with the results of the analytic theory according to which fourth-order processes can saturate the explosive growth of the hexagon instability only in this region. However, in this case the analytical $B_k^{\rm an}$ and numerical $B_k^{\rm num}$ values of the light-beam amplitudes differ rather strongly: $|B_k^{\rm num}|/|B_k^{\rm an}||_{z=0} \sim 2$, which indicates a strong renormalization of the amplitudes of the hexagons due to higher-order wave processes. Thus, the predictions of the four-wave theory are valid more qualitatively than quantitatively. For $n_0L/l \gtrsim 0.1$, when the four-wave interactions surely cannot ensure saturation of the explosive instability, the nonlinearity increases with increasing n_0L/l.

Additional numerical investigations showed that, since the amplitudes of the higher-order harmonics rapidly decay as their labels increase, if we assume by definition that all the higher-order combination harmonics equal zero but take into account all possible processes between the 0, 1, 2, $\sqrt{3}$ harmonics, the amplitude of the fundamental harmonic changes by more than 2%. Thus, for the strongly nonlinear theory it actually turns out to be sufficient to take into account wave processes up to eighth order, while including in those processes only interactions with the participation of harmonics 0, 1, 2, $\sqrt{3}$. Note also that only harmonics 0, 1, 2, $\sqrt{3}$ are observed in experiment, while the higher harmonics are too weak to be recorded (see, e.g., Refs. 6 and 8). In these experiments the intensity of hexagons is observed to be from one to three percent of the intensity of the pump, which is somewhat lower than the results obtained from the numerical experiment, which gives a value $|B_k(0)|^2 \simeq 0.04$. This is probably explained by the fact that losses due to reflection at the crystal faces (of order 15% for light incident on the back face of the crystal and just as much again when the light reenters the crystal after reflection from the feedback mirror) have not been included in the system (19), (25), and losses in the reflection of light from the feedback mirror have also been neglected.

We mention in conclusion that for $n_0L/l \gtrsim 0.85$ stationary hexagon solutions turn out to be unstable against repumping of energy back into the $\sqrt{3}$ harmonic. This instability is connected with the fact already noted in Sec. 3 that for $n_0L/l \simeq 1.43$ the depths of the first and second minima of the threshold curve $\gamma_i^{\rm min}(k_dl)$ for the linear instability are comparable (see Fig. 3a). In this case the ratio $k_d^{\rm min}|_{m=2}/k_d^{\rm min}|_{m=1}$ is close to 3 (accurate to 2%). Thus, in the neighborhood of $n_0L/l \sim 1.43$ the amplitudes of the first-order and $\sqrt{3}$ harmonics are the same order, and hence they are coupled by the three-wave interaction. This case requires the inclusion of all wave processes up to eight-wave in the numerical calculations, and thus the treatment of a larger number of harmonics than were included in the numerical experiment described above. Consideration of this problem lies outside the framework of this paper.

8. CONCLUSION

Thus, the following results have been obtained in this paper. A system of equations (19) has been derived with boundary conditions (25) that describes the evolution of the sideband wave amplitudes and space-charge field for an arbitrary level of nonlinearity. Linearization of this system leads to the threshold condition (28) for appearance of a transverse instability, which exactly coincides with the results of Ref. 12. It has been shown that the threshold curve $\gamma_i(k_dl)$ consists of a sequence of minima whose relative depth changes with the parameter n_0L/l, which is proportional to the distance L to the feedback mirror. For $n_0L/l < 1.43$ the deepest minimum (i.e., corresponding to the lowest instability threshold) turns out to be the first, and as the quantity n_0L/l increases the second, third, etc., minima become the deepest in succession. Expression (30) was obtained, which describes with high accuracy the position of all the minima. In this case the magnitudes of the transverse

wave vectors belong to the set 1, $\sqrt{3}$, $\sqrt{5}$,... for the first, second, third, etc. minima. Moreover, a set of explicit solutions (29) has been found for the threshold Eq. (28) which correspond to the deepest values of the minima for all possible values of the parameter n_0L/l. Eigenvectors were calculated for the direct linear boundary value problem (25), (26) and its Hermitian conjugate (36), (35) at the instability threshold as functions of n_0L/l. For the special cases (29) explicit analytic expressions (33), (37) were given for these vectors.

For small values of the supercritical parameter h, when the sideband beams are unstable only within a narrow ring $|\mathbf{k}| \simeq \sqrt{2k_d^{\min}k_0n_0}$, the general solution to the nonlinear boundary value problem (19), (25) was reduced (by expanding (38) in eigenfunctions of the linear problem) to the system of amplitude equations (3). This system consists of a Landau expansion in the amplitude of the growing linear modes. The matrix elements U and $T_{kk_1k_2k_3}$ for three- and four-wave interactions respectively were calculated at the instability threshold as functions of n_0L/l. These matrix elements turn out to be purely real quantities. In the special case (29) the explicit analytic expression (41) was obtained for U. The fact that the matrix element U for the three-wave interaction differs from zero is of fundamental importance, since it leads to the appearance of the explosive three-wave instability and correlation of sideband waves whose wave-vectors make angles with one another that are multiples of $\pi/3$.

The possibility of stabilization of explosive growth of the hexagons due to four-wave interactions was investigated, Eqs. (44) were obtained to describe the temporal dynamics of generation of the steady-state hexagonal solutions (46), and the stability condition (47) for these solutions was found. As a result it was shown that for $n_0L/l \lesssim 0.1$ four-wave interactions can saturate the explosive instability. Outside this region it is definitely necessary to take into account higher-order wave processes. A numerical experiment was performed to investigate the nonlinear boundary value problem (19), (25). It was shown that in general it is necessary to take into account all wave processes up to eight-wave. However, among these processes the only important ones were interactions between the fundamental harmonic and harmonics 0, $\sqrt{3}$, and 2. For $n_0L/l \lesssim 0.1$ the results obtained agreed quantitatively with the results of the four-wave interaction theory; however, it was found that higher-order wave processes lead to a substantial renormalization of the hexagon amplitudes given by the analytic expression (46). It was shown that for $n_0L/l \gtrsim 0.85$ the strongly nonlinear stationary hexagonal solutions (obtained in the numerical experiment) become unstable against repumping of energy into higher harmonics. The reason for this is that in this region the fundamental harmonic and $\sqrt{3}$ harmonic are of the same order due to the closeness of their linear instability thresholds. In this case the transverse wave vectors of these two harmonics correspond to positions of two successive minima of the threshold curve $\gamma_i(k_dl)$, which leads to an intense exchange of energy between them.

In conclusion the author thanks E. A. Kuznetsov for posing the problem and for useful discussions. This work was carried out with the support of the Russian Fund for Fundamental Research (Grant 97-01-00093), the program of government support for leading scientific schools (Grant 96-15-96093), the Landau Scholarship Fund, KFA, Forschungzentrum, Juelich, Germany, and the INTAS Fund (Grant 96-0954).

*)E-mail: lushniko@landau.ac.ru

[1] J. Pender and L. Hesselink, J. Opt. Soc. Am. B **7**, 1361 (1990).
[2] A. Petrossian, M. Pinard, A. Maître, J.-Y. Courtois, and G. Grynberg, Europhys. Lett. **18**, 689 (1992).
[3] R. MacDonald and H. J. Eichler, Opt. Commun. **89**, 289 (1992).
[4] M. Tamburrini, M. Bonavita, S. Wabnitz, and E. Santamato, Opt. Lett. **18**, 855 (1993).
[5] J. V. Moloney and A. C. Newell, *Nonlinear Optics* (Addison-Wesley, Reading MA, 1992).
[6] T. Honda, Opt. Lett. **18**, 598 (1993).
[7] P. P. Banerjee, H.-L. Yu, D. A. Gregory, N. Kukhtarev, and H. J. Caulfield, Opt. Lett. **20**, 10 (1995).
[8] T. Honda and A. Matsumoto, Opt. Lett. **20**, 1755 (1995).
[9] N. V. Kukhtarev, T. Kukhtareva, H. J. Caulfield, P. P. Banerjee, H.-L. Yu, and L. Hesselink, Opt. Eng. (Bellingham) **34**, 2261 (1995).
[10] *Photorefractive Materials and Their Applications*, P. Günter and J.-P. Huignard eds. (Springer–Verlag, Berlin, 1988); M. P. Petrov, S. I. Stepanov, and A. V. Khomenko, *Photorefractive Crystals in Coherent Optical Systems* (Nauka, St. Petersburg, 1992; Springer, New York, 1991).
[11] W. J. Firth and C. Paré, Opt. Lett. **13**, 1096 (1988); G. D'Alessandro and W. J. Firth, Phys. Rev. Lett. **66**, 2597 (1991).
[12] T. Honda and P. P. Banerjee, Opt. Lett. **21**, 779 (1996).
[13] B. I. Sturman and A. I. Chernykh, Zh. Éksp. Teor. Fiz. **111**, 1611 (1997) [JETP **84**, 881 (1997)].
[14] L. D. Landau and E. M. Lifshits, *Fluid Mechanics* (2nd ed. Pergamon Press, Oxford, 1987) [Russ. original Nauka, Moscow, 1988].
[15] B. I. Sturman and V. M. Fridkin, *The Photovoltaic and Photorefractive Effects in Noncentrosymmetric Materials* (Nauka, Moscow, 1992); (Gordon & Breach, New York, 1992); B. I. Sturman, S. G. Odulov, and M. Yu. Goulkov, Phys. Rep. **275**, 197 (1996).
[16] N. V. Kukhtarev, Pis'ma Zh. Tekh. Fiz. **2**, 1114 (1976) [Sov. Tech. Phys. Lett. **2**, 438 (1976)].
[17] M. Saffman, A. A. Zozulya, and D. Z. Anderson, J. Opt. Soc. Am. B **11**, 1409 (1994).
[18] E. A. Kuznetsov and M. D. Spektor, Zh. Éksp. Teor. Fiz. **71**, 262 (1976) [Sov. Phys. JETP **44**, 136 (1976)].
[19] E. A. Kuznetsov and M. D. Spektor, Appl. Math. Theor. Phys. **2**, 76 (1980) [in Russian].

Translated by Frank J. Crowne